

# The balloon-borne large-aperture submillimeter telescope for polarimetry: BLAST-Pol

Laura M. Fissel<sup>a</sup>, Peter A. R. Ade<sup>b</sup>, Francesco E. Angilè<sup>c</sup>, Steven J. Benton<sup>d</sup>,  
Edward L. Chapin<sup>e</sup>, Mark J. Devlin<sup>c</sup>, Natalie N. Gandilo<sup>a</sup>, Joshua O. Gundersen<sup>f</sup>,  
Peter C. Hargrave<sup>b</sup>, David H. Hughes<sup>g</sup>, Jeffrey Klein<sup>c</sup>, Andrei L. Korotkov<sup>h</sup>, Galen Marsden<sup>e</sup>,  
Tristan G. Matthews<sup>i</sup>, Lorenzo Moncelsi<sup>b</sup>, Tony K. Mroczkowski<sup>c</sup>, C. Barth Netterfield<sup>a,d</sup>,  
Giles Novak<sup>i</sup>, Luca Olmi<sup>j,k</sup>, Enzo Pascale<sup>b</sup>, Giorgio Savini<sup>l</sup>, Douglas Scott<sup>e</sup>, Jamil A. Shariff<sup>a</sup>,  
Juan Diego Soler<sup>a</sup>, Nicholas E. Thomas<sup>f</sup>, Matthew D. P. Truch<sup>c</sup>, Carole E. Tucker<sup>b</sup>,  
Gregory S. Tucker<sup>h</sup>, Derek Ward-Thompson<sup>b</sup>, Donald V. Wiebe<sup>e</sup>

<sup>a</sup>Department of Astronomy & Astrophysics, University of Toronto, 50 St. George Street,  
Toronto, ON M5S 3H4, Canada; <sup>b</sup>Department of Physics & Astronomy, Cardiff University, 5  
The Parade, Cardiff, CF24 3AA, UK;

<sup>c</sup>Department of Physics and Astronomy, University of Pennsylvania, 209 South 33rd Street,  
Philadelphia, PA 19104;

<sup>d</sup>Department of Physics, University of Toronto, 60 St. George Street, Toronto, ON M5S 1A7,  
Canada;

<sup>e</sup>Department of Physics & Astronomy, University of British Columbia, 6224 Agricultural  
Road, Vancouver, BC V6T 1Z1, Canada;

<sup>f</sup>Department of Physics, University of Miami, 1320 Campo Sano Drive, Coral Gables, FL  
33146;

<sup>g</sup>Instituto Nacional de Astrofísica Óptica y Electrónica (INAOE), Aptdo. Postal 51 y 72000  
Puebla, Mexico;

<sup>h</sup>Department of Physics, Brown University, 182 Hope Street, Providence, RI 02912;

<sup>i</sup>Department of Physics and Astronomy, Northwestern University, 2145 Sheridan Road,  
Evanston, IL 60208-3112;

<sup>j</sup>University of Puerto Rico, Rio Piedras Campus, Physics Dept., Box 23343, UPR station, San  
Juan, Puerto Rico;

<sup>k</sup>Osservatorio Astrofisico di Arcetri, INAF, Largo E. Fermi 5, I-50125, Firenze, Italy.;

<sup>l</sup>Department of Physics and Astronomy, University College London, Gower Street, London,  
WC1E 6BT, UK;

## ABSTRACT

The Balloon-borne Large Aperture Submillimeter Telescope for Polarimetry (BLAST-Pol) is a suborbital mapping experiment designed to study the role played by magnetic fields in the star formation process. BLAST-Pol is the reconstructed BLAST telescope, with the addition of linear polarization capability. Using a 1.8 m Cassegrain telescope, BLAST-Pol images the sky onto a focal plane that consists of 280 bolometric detectors in three arrays, observing simultaneously at 250, 350, and 500  $\mu\text{m}$ . The diffraction-limited optical system provides a resolution of 30'' at 250  $\mu\text{m}$ . The polarimeter consists of photolithographic polarizing grids mounted in front of each bolometer/detector array. A rotating 4K achromatic half-wave plate provides additional polarization modulation. With its unprecedented mapping speed and resolution, BLAST-Pol will produce three-color polarization maps for a large number of molecular clouds. The instrument provides a much needed bridge in spatial coverage between

---

Further author information: (Send correspondence to L. M. Fissel)

L. M. Fissel: E-mail: fissel@astro.utoronto.ca, Telephone: 416-946-0946

larger-scale, coarse resolution surveys and narrow field of view, and high resolution observations of substructure within molecular cloud cores. The first science flight will be from McMurdo Station, Antarctica in December 2010.

**Keywords:** submillimeter — stars: formation — instrumentation: miscellaneous — balloons — polarization — dust emission

## 1. INTRODUCTION

BLAST-Pol, the Balloon-borne Large Aperture Submillimeter Telescope for Polarimetry, is a stratospheric 1.8 m telescope which maps linearly polarized submillimeter emission with bolometric detectors operating in three 30% wide bands at 250, 350, and 500  $\mu\text{m}$ . BLAST-Pol's diffraction-limited optics were designed to provide a resolution of 30'', 42'', and 60'' at the three wavebands, respectively. The detectors and cold optics are adapted from those used by the SPIRE instrument on Herschel.<sup>1</sup>

BLAST-Pol is a rebuilt and enhanced version of the BLAST telescope,<sup>2</sup> with added linear polarization capability. BLAST was designed to conduct confusion-limited, wide-area extragalactic and Galactic surveys at submillimeter (submm) wavelengths from an balloon platform.

BLAST had two Long Duration Balloon (LDB) flights. The first was a 4-day flight from Kiruna, Sweden in June of 2005 (BLAST05). Unfortunately the telescope was found to be out of focus, due to slight damage of the primary mirror during the launch or ascent, so the telescope was restricted to observing bright Galactic targets. BLAST was repaired and flown again from Antarctica in December 2006 for 11 days (BLAST06). For BLAST06 the instrument worked perfectly and multiple deep, large-area maps were obtained for Galactic and extra-galactic fields.

After termination of the Antarctic flight the parachute could not be detached, which resulted in the payload being dragged  $\sim 200$  km along the ground in 24 hours. BLAST was largely destroyed, but fortunately the pressure vessel containing the hard drives which stored all of the experiment data was recovered. In addition, the mirrors, detectors and receiver were all recovered, and have been used in the construction of BLAST-Pol.

The BLAST telescope has left a legacy of fantastic science results. BLAST provided the first deep, wide area maps at 250, 350 and 500  $\mu\text{m}$ , bands that are very difficult or often impossible to observe from even the best ground based sites in the world. Some science highlights include measurement of the FIR background at 250, 350 and 500  $\mu\text{m}$ , including a 0.8  $\text{deg}^2$  confusion-limited map in the GOODS South region, where it was shown that more than half of the FIR background light originates in galaxies at redshift  $> 1.2$ ,<sup>3–5</sup> the first determination of deep, extragalactic number counts at these wavelengths,<sup>6</sup> the detection of clustering in the far-IR background,<sup>7</sup> three-band resolved sub-mm images of several nearby galaxies,<sup>8</sup> and the determination of luminosities, masses and temperatures of more than a thousand compact sources in the Vela Molecular cloud, which may form into stars.<sup>9</sup>

With the addition of a polarimeter, BLAST has now been transformed into BLAST-Pol, a uniquely sensitive polarimeter for probing linearly polarized Galactic dust emission. BLAST-Pol will map the magnetic field structure of many different star-forming regions. These maps will provide a fantastic data set for addressing what role magnetic fields play in the star formation process, an important outstanding question in our understanding of how stars form. BLAST-Pol will be able to map magnetic fields across entire Giant Molecular Clouds (GMCs), with sufficient resolution to probe fields in dense filamentary sub-structures and molecular cores. The experiment provides a crucial bridge between the large area but coarse resolution polarimetry provided by experiments such as Planck (5' resolution) with the resolution of the ALMA telescope.

BLAST-Pol's first flight is scheduled for December 2010 from McMurdo Station, Antarctica.

## 2. SCIENCE GOALS

### 2.1 Probing the Role of Magnetic Fields in Star Formation

Many fundamental questions about the process of star formation remain unanswered.<sup>10</sup> Is star formation regulated by magnetic fields or by turbulence? How long does the star formation process last? Do molecular clouds

and their associated substructures (dense cores, filaments, and clumps), have lifetimes exceeding their turbulent crossing times? What determines the final masses of stars?

It is difficult to observe magnetic fields in molecular clouds.<sup>11,12</sup> One promising method for probing them is to observe clouds with a far-IR/submm polarimeter.<sup>13,14</sup> By tracing the linearly polarized thermal emission from dust grains aligned with respect to the local magnetic fields, we can measure the direction of the plane-of-the-sky component of the magnetic field within the cloud. By mapping polarization we can therefore trace the magnetic field direction across entire molecular clouds.

Far-IR/submm polarimetry is an emerging area of star formation research, with many upcoming experiments that will map fields on different scales. Planck<sup>15</sup> will provide coarse resolution (FWHM  $\sim 5'$ ) submm polarimetry maps of the entire sky. ALMA will provide sub-arcsecond resolution polarimetry capable of resolving fields within cores and disks, but will not be sensitive to cloud-scale fields. BLAST-Pol, with a  $30''$  FWHM beam at  $250\mu\text{m}$ , will be the first submm polarimeter to have both the sensitivity and mapping speed necessary to trace fields across entire clouds for a statistically significant sample of molecular clouds, and sufficient spatial resolution to track the cloud fields into the dense substructures and cores within the clouds. Observations from the SPARO experiment show that extended submm emission from giant molecular clouds (GMCs), where most stars are thought to have formed, is indeed polarized<sup>16,17</sup> (Fig. 1). BLAST-Pol will map polarized emission over a wide range of dust column densities corresponding to  $A_v \geq 4$ , yielding  $\sim 1000$  independent polarization detections per cloud, for dozens of clouds.

The BLAST-Pol maps will allow us to make the first detailed comparisons between observed molecular cloud field maps and synthetic maps. The latter can be derived from numerical simulations of molecular clouds (for example see Ref. 18). This will allow us to make detailed observational tests of theoretical magneto-hydrodynamic (MHD) models of star formation.

In particular, we will address the following questions with BLAST-Pol:

1. *Is molecular core morphology determined by large-scale magnetic fields?* Jones & Basu<sup>19</sup> have argued that observations show a predominance of oblate-shaped cores in molecular clouds, as has been predicted by magnetically-regulated models of core collapse.<sup>20,21</sup> These models also predict that each core should be embedded in a large-scale cloud field which runs parallel to the core's minor axis. Submm polarimetry observations of 4 quiescent cores with SCUBA<sup>14</sup> questioned this prediction by finding that the magnetic fields were misaligned, and therefore more consistent with turbulence dominated magnetic models. More recently Tassis et al.<sup>22</sup> analyzed observations of 24 clouds taken with the Hertz polarimeter at the Caltech Submillimeter Observatory (CSO) and found in their statistical analysis that models with oblate cores and mean magnetic field orientations with small deviations from the core minor axis are preferred. However, observations of more clouds are needed in order to reject models. Also, Hertz, SCUBA (and SCUBA-2) cannot realistically detect fields in lower density regions: what is needed are observations tracing core fields out into the surrounding lower-density cloud environment. BLAST-Pol will provide these for a large sample of molecular clouds.
2. *Do filamentary structures within clouds have magnetic origins?* Faint, low column density  $^{12}\text{CO}$  filaments observed in Taurus<sup>23,24</sup> seem to closely follow magnetic field lines traced by optical polarimetry, which could indicate streaming of molecular gas along field lines. However, denser filaments in Taurus and some other clouds show no preferred orientation with respect to the field direction traced by nearby polarimetry pseudo-vectors from optical observations of background stars.<sup>25</sup> This may imply a non-magnetic origin for the denser filaments, or it may simply reflect the inadequacies of optical/near-IR polarimetry for tracing fields in dense, shielded regions within molecular clouds.<sup>12,26</sup> In contrast, optical polarization observations of the Pipe Nebula<sup>27</sup> show that the local magnetic field is perpendicular to the filamentary structure. We will use BLAST-Pol to map dense filaments to answer questions about the relationship between fields and cloud sub-structures.
3. *How strong are magnetic fields in molecular clouds, and how does the field strength vary from cloud to cloud?* Simulations have shown that clouds where magnetic fields are strong enough to play an important role in supporting the cloud against gravitational collapse tend to have aligned polarization angles, where as clouds

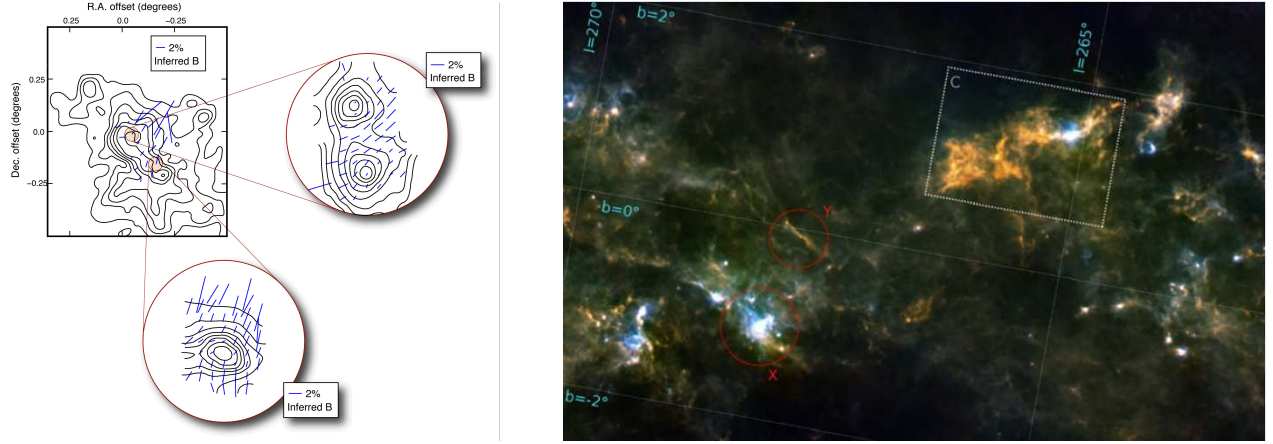


Figure 1. *Left:* Submillimeter polarimetry (at  $450\ \mu\text{m}$ ) of NGC 6334, a massive GMC at a distance of 1700 pc. The pseudo-vectors in the map at upper left were obtained using the SPARO instrument at the South Pole, and the “blowup” images at the right and bottom are from Hertz/CSO observations on Mauna Kea at  $350\ \mu\text{m}$ .<sup>17</sup> The orientation of each pseudo-vector shows the inferred field direction, with the length of each line proportional to the degree of polarization. *Right:* A excerpt from a  $50\ \text{deg}^2$  false color BLAST06 map of the Vela Molecular Cloud complex.<sup>9</sup> Vela C, a GMC located at a distance of  $\sim 700$  pc and a planned BLAST-Pol target, is indicated with a dashed rectangle. During the first BLAST-Pol flight, we will map  $\sim 20$  such clouds, obtaining  $\sim 1000$  polarization pseudo-vectors per cloud.

with more randomly oriented polarization angles imply weaker fields.<sup>18</sup> Field strength can be estimated using the Chandrasekhar-Fermi (CF) technique,<sup>28</sup> which relates dispersion in polarization angle to field strength.<sup>28,29</sup> CF field strength estimates for molecular cloud cores have been obtained from submm data, and the derived magnetic field strengths are in rough agreement those derived from Zeeman observations.<sup>11</sup> Numerical turbulence simulations have been used to calibrate the CF technique for molecular clouds.<sup>18,30,31</sup> BLAST-Pol will determine the power spectrum of the polarization angle dispersion over a large range of spatial scales, for dozens of molecular clouds. These data should lead to improved models and better CF calibration. BLAST-Pol will also measure 3-color polarization spectra variations within the cloud,<sup>32,33</sup> which will allow us to explore the dust properties and temperature structure of each cloud. Our observations will probe the dependence of field strength on cloud age, location, and mass.

## 2.2 Polarized Galactic Dust Foregrounds

The search for primordial gravitational waves through detecting the B-mode polarization of the Cosmic Microwave Background (CMB)<sup>34–36</sup> requires precise control of instrumental and astrophysical systematics at a level which allows the detection of this extremely faint signal. WMAP polarization observations<sup>37</sup> clearly demonstrate that polarized foregrounds caused by diffuse Galactic dust emission are likely to be comparable or larger than the B-mode CMB polarization anisotropy at large angular scales (multipoles  $\ell < 100$ ) and at intermediate Galactic latitudes. This situation differs from the CMB temperature anisotropy signal where most of the sky is dominated by the CMB. It requires significant foreground emission modeling in order to extract the underlying CMB polarization signal.

Most of the polarized Galactic foregrounds observed by WMAP are due to synchrotron emission, but at the highest WMAP frequency band (94 GHz), there is evidence for polarized dust emission. This polarized dust emission is potentially problematic for many higher-frequency bolometric CMB polarization experiments (for example EBEX, Spider, Clover, QUAD, BICEP, Keck, Planck-HFI, and Polarbear), since the emission is expected to rise significantly with frequency as predicted by models based on observations at  $100\ \mu\text{m}$ . The ARCHEOPS balloon mission measured Galactic dust polarization on scales of  $15'$  at submm wavelengths. ARCHEOPS results<sup>38</sup> have shown that radiation from diffuse Galactic dust is polarized (as expected) at the 3–5% level, but in some regions the polarization is as high as 10%. While these measurements were made near the Galactic plane, they point to the need for more information at higher latitudes, with higher sensitivity, better angular resolution,

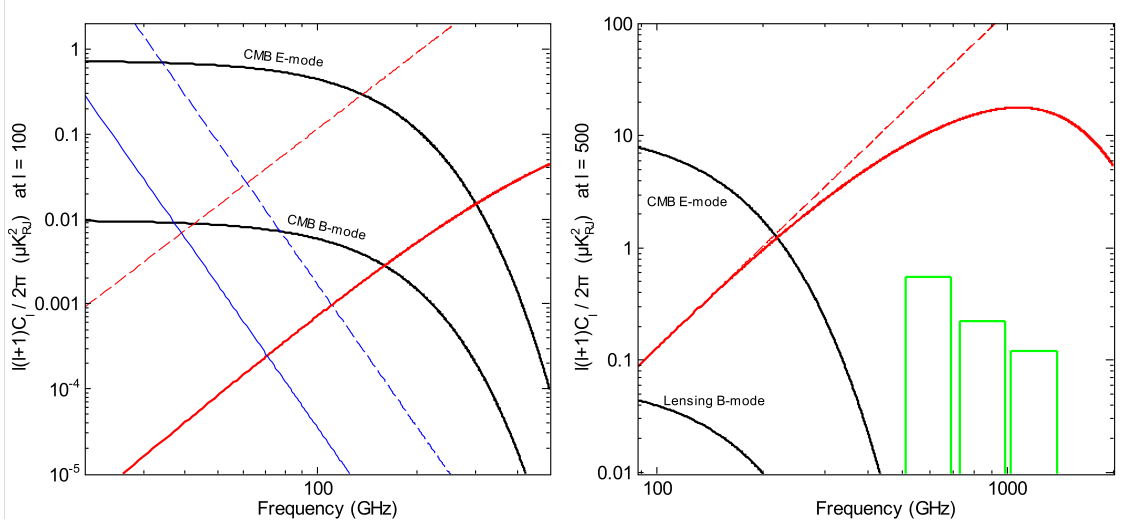


Figure 2. *Left:* The spectrum of B-mode foregrounds from Galactic dust (red) and synchrotron (blue) expected outside WMAP’s P06 mask<sup>37</sup> (dashed), and from a selected sky region (solid), compared with the E and B-mode CMB (black, solid). These are all at  $\ell = 100$  and in antenna temperature units. This dust model assumes model 8 from Finkbeiner et al. (1999).<sup>39</sup> *Right:* A similar plot at  $\ell = 500$ . The green bars show the BLAST-Pol noise at a resolution of  $8'$  from a 48-hr observation of  $0.5 \text{ deg}^2$ . At these angular scales, the CMB signal is dominated by the lensing B-modes. The Galactic dust signal, normalized to WMAP, peaks at the BLAST-Pol frequencies. (The CMB models here assume a standard  $\Lambda$ CDM cosmology with  $r = 0.1$ .)

and at multiple wavelengths. Despite the WMAP and Archeops results, no information exists for any region of the sky at the accuracy required for a B-mode signal detection, and very little information exists at frequencies relevant to CMB science (at least until Planck results are published).

There are additional puzzles in dust polarimetry that must be resolved if anyone is to make a robust detection of the CMB B-modes. For example, polarimetry of bright molecular cloud cores at  $350 \mu\text{m}$  and  $1 \text{ mm}$  has revealed the surprising result that the polarization fraction at  $1 \text{ mm}$  is larger by a factor of  $\sim 2$  compared to that at  $350 \mu\text{m}$ .<sup>13</sup> The Planck satellite will provide a unique data set by mapping the sky with polarization-sensitive bolometers in bands centered from  $850 \mu\text{m}$  to  $3 \text{ mm}$ . The  $850 \mu\text{m}$  band will provide an unparalleled data set for studying polarized dust emission. In addition to Planck, balloon-borne and other ground-based instruments employ anywhere between 2 to 6 frequency bands to assist in discriminating against foreground contamination. But the ability to separate the foreground dust emission to the necessary level to detect B-mode polarization depends on the complexity of the polarized dust emission.

Figure 2 shows the expected polarized dust emission as measured by the 3 yr WMAP data<sup>37</sup> and the level of foregrounds predicted in a selected  $\sim 200 \text{ deg}^2$  sky region ( $l = 258^\circ$ ,  $b = -46^\circ$ ) accessible by sub-orbital and ground-based instruments. Amazingly, the dust signal extrapolated to the CMB frequencies is comparable to the gravitational-wave contribution  $r=0.1$  B-mode signal level that is being probed by the current generation of experiments. For this reason, it is imperative that we begin to understand high-latitude polarized dust emission. Given these rather low signal levels, BLAST-Pol will be limited in its ability to conduct large surveys that could be used as templates for lower frequency CMB polarization observations. However, a 48-hr survey over a  $0.5 \text{ deg}^2$  sky region (Fig. 2, right panel) will enable BLAST-Pol to constrain dust properties which are difficult to measure at lower frequencies. In particular, the determination of dust temperature and degree of polarization will be highly degenerate as measured by all CMB experiments in the Rayleigh-Jeans tail of the dust spectrum. On the other hand, the ability of BLAST-Pol to extract these parameters will be straightforward, since the measurements are made near the peak of the cold dust spectrum.

The first of our two maps will be aimed at a very low dust emission region, comparable to  $1 \text{ MJy sr}^{-1}$  at  $100 \mu\text{m}$ , that is ideally coincident with a deep CMB polarization measurement. The other will occur in

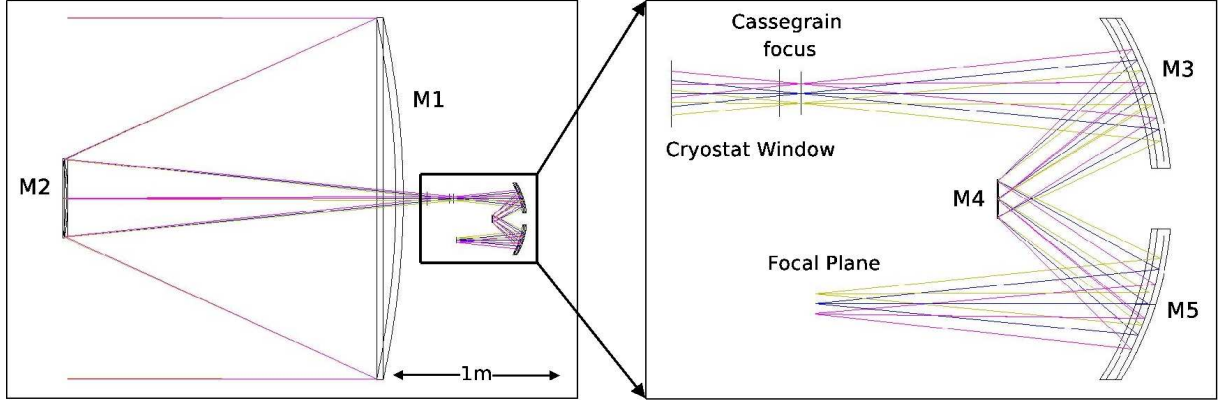


Figure 3. Schematic of the optical layout for the BLAST telescope and receiver is shown on the left, with the 1.5 K optics, located within the cryostat, shown in an expanded view on the right. The image of the sky formed at the input aperture is re-imaged onto the bolometer detector array at the focal plane. The mirror M4 serves as a Lyot stop, which defines the illumination of the primary mirror for each element of the bolometer detector arrays. The three wavelength bands are separated by a pair of dichroic beamsplitters (not shown) which are arranged in a direction perpendicular to the plane, between M5 and the focal plane.

a mid-latitude region with a higher dust brightness that will almost certainly be sampled by Planck. The corresponding higher signal will enable parameter extraction without the aid of lower frequency CMB polarization measurements.

When these measurements are combined, they will enable the characterization of the spatial variation of the polarization percentage, dust temperature, and dust emissivity. While the maps will be smoothed to relatively large pixels for comparison with Planck, we will retain the ability to see any fine-scale, higher-level polarization signals to help the planning of future ground-based, balloon-borne and space experiments.

### 3. INSTRUMENT

#### 3.1 Optical Design

BLAST-Pol utilizes a Cassegrain telescope consisting of a 1.8 m parabolic primary mirror (M1) and a 40 cm correcting secondary (M2). The field of view of the telescope at  $250\ \mu\text{m}$  is  $13.5' \times 6.5'$  at the Cassegrain focus. This system redirects the light to a series of cryogenically cooled (1.5 K) re-imaging optics (M3, M4, M5) arranged in an Offner-relay configuration, where M4 is a Lyot stop. Figure 3 shows a schematic of the optical path of the BLAST telescope.

Radiation emerging from M5 is split into three frequency bands by low-pass edge dichroic filters,<sup>40</sup> which allows us to image the sky simultaneously at 250, 350 and  $500\ \mu\text{m}$ . The first dichroic filter reflects wavelengths shorter than  $300\ \mu\text{m}$  and transmits longer wavelengths. This reflected light is directed on to a filter directly in front of the  $250\ \mu\text{m}$  array, which reflects wavelengths shorter than  $215\ \mu\text{m}$ , and is further defined by the waveguide frequency cutoff at the exit of each of the feedhorns coupled to the detector array. For the 350 and  $500\ \mu\text{m}$  arrays, the band is defined at the short-wavelength end by the transmission of a dichroic filter and at the long-wavelength end by the waveguide cutoff. Each band has a 30% width. The frequency performance of the filters was evaluated with Fourier transform spectroscopy.

Although the primary mirror was recovered after the destruction of BLAST06, eventually it was decided that a new primary mirror was needed. The surface of the new mirror has an RMS of  $\sim 1.0\ \mu\text{m}$ , with the overall shape of the mirror good to  $\sim 10\ \mu\text{m}$ . The secondary mirror was also recovered after BLAST06, and has been reused for BLAST-Pol (after resurfacing to remove some scratches). The estimated antenna efficiency of the telescope is  $> 80\%$ , with losses caused by both the roughness of the primary and the quality of the re-imaging optics. More information about the optical design and performance of the BLAST telescope can be found in Refs. 41 and 2.

Temperatures of the primary and secondary mirrors do not remain constant throughout the flight. Diurnal temperature variations of  $\sim 10^\circ\text{C}$  have been observed on previous BLAST flights.<sup>2</sup> These thermal variations result in changes to the radii of curvature of various optical surfaces. To compensate, the position of the secondary mirror with respect to the primary can be changed in flight by three stepper motor actuators. These actuators are also used to set the original tip/tilt alignment of the secondary. Analysis of the BLAST optical system indicates that the distance between the primary and secondary mirrors must be kept to within  $100\ \mu\text{m}$  to avoid significant image degradation.

### 3.2 Detectors

The BLAST-Pol focal plane consists of 149, 88 and 43 detectors at 250, 350 and  $500\ \mu\text{m}$  respectively. The detectors consist of silicon-nitride micromesh (“spider-web”) bolometric detectors coupled with  $2f\lambda$  feedhorn arrays. The bolometer detector array design is based on the Herschel SPIRE instrument detectors.<sup>42,43</sup> Detector sensitivity is limited by photon shot-noise from the telescope. The total emissivity for the warm optics of  $\sim 6\%$  is dominated by blockage from the secondary mirror and supports.

The detectors are read out with an AC-biased differential circuit. The data acquisition electronics demodulate the detector signals to provide noise stability to low frequencies ( $< 30\ \text{mHz}$ ), which allows the sky to be observed in a slowly-scanned mode. Slow scanning is preferable to a mechanical chopper for mapping large regions of sky. The data are collected using a high-speed, flexible, 22-bit data acquisition system developed at the University of Toronto. The system can synchronously sample up to 600 channels at any rate up to  $4\ \text{kHz}$ . Each channel consists of a buffered input and a sigma-delta analog to digital converter. The output from 24 channels are then processed by an Altera programmable logic device which digitally anti-alias filters and demodulates each input. The results then are stored to disk.

### 3.3 Polarimetry

A photo-lithographed polarizing grid has been mounted in front of the feed-horn arrays for each bolometer detector array. The grids are patterned to alternate the polarization angle sampled by  $90^\circ$  from horn-to-horn and thus bolometer-to-bolometer along the scan direction. BLAST-Pol will scan so that a source on the sky passes along a row of detectors, and thus the time required to measure one Stokes parameter ( $Q$  or  $U$ ) is just equal to the separation between bolometers divided by the scan speed. For the  $250\ \mu\text{m}$  detector array where the bolometers are separated by  $45''$ , and assuming a typical scan speed of  $0.1^\circ$  per second, this time would be 0.125 seconds. This timescale is short compared to the characteristic low frequency ( $1/f$ ) noise knee for the detectors at  $0.035\ \text{mHz}$ .<sup>2</sup>

In order to measure the other Stokes parameter and provide polarization modulation an Achromatic Half Wave Plate (AHWP) has been incorporated into the optical design as shown in Figure 4. The HWP is mounted inside the optics box  $19.1\ \text{cm}$  from the Cassegrain focus of the telescope to minimize the modulation of any potential plate local defects. The predicted modulation efficiency across the BLAST bands is given in Figure 5.

The use of a rotating HWP as a polarization modulator is a widespread technique at millimeter and submillimeter wavelengths (see for example Refs. 44, 45, 46 and 47). The BLAST-Pol HWP is  $10\ \text{cm}$  in diameter and is constructed from 5 layers of sapphire, each  $500\ \mu\text{m}$  in thickness. The layers are glued together with a  $6\ \mu\text{m}$  layer of polyethylene, and an anti-reflection coating (made from metal mesh filter technology, see Ref. 48) is glued to each surface of the half-wave plate. Figure 5 shows the predicted transmissions and modulation efficiencies for the BLAST HWP as a function of frequency. They are based on a comprehensive set of data taken at room temperature, which has been extrapolated to estimate the  $4\ \text{K}$  performance of the HWP.

We operate the HWP in a stepped mode, rather than a continuously rotating mode. The rotator employs a pair of thin-section steel ball bearings housed in a stainless steel structure, and is driven via a gear train and a G-10 shaft leading to a stepper motor outside the cryostat. A ferrofluidic vacuum seal is used for the drive shaft. The angle sensing at liquid Helium temperatures is accomplished by a potentiometer element making light contact with phosphor bronze leaf springs. During operation, we will carry out spatial scans at eight HWP angles spanning  $180$  degrees of rotation ( $22.5^\circ$  steps). The rotator and encoder are based on a design used successfully at South Pole.<sup>49</sup>



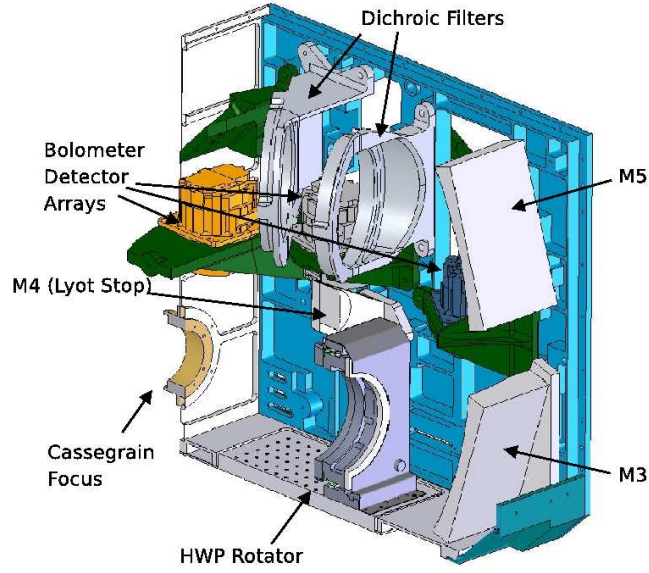


Figure 4. A cutaway view of the BLAST-Pol optics box. The light enters from the lower left and is re-imaged onto the bolometer detector arrays (BDAs). Dichroic filters split the beam into each of the BDAs for simultaneous imaging of the sky at 250, 350 and 500  $\mu\text{m}$ . A modulating half-wave plate is mounted between the entrance to the optics box and M3, and polarizing grids have been mounted directly in front of each of the BDAs. The stepper motor which rotates the waveplate is located outside the optics box.

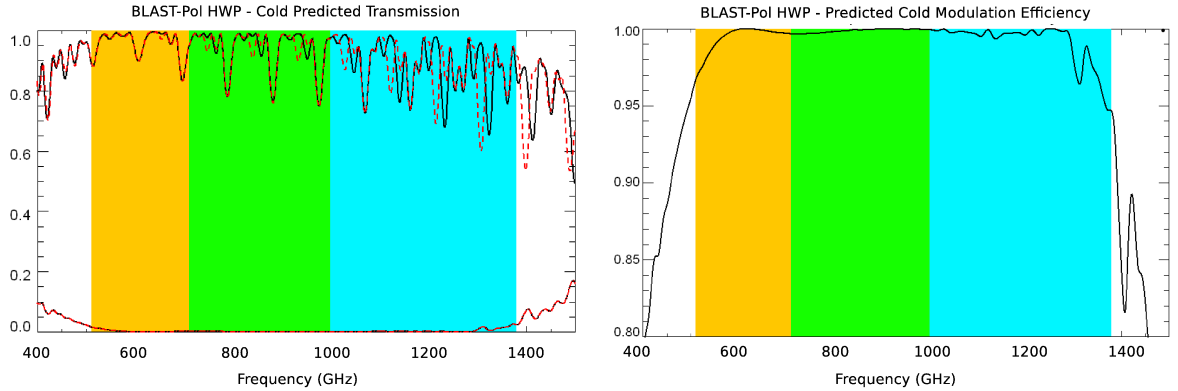


Figure 5.

*Left:* The predicted transmissions through the HWP as a function of frequency. The approximate extent of the BLAST bandpasses are also indicated. Solid Black Curve: transmission between two parallel polarizers (i.e.  $Q=1$  to  $Q=1$ ) with the HWP axis at 0 deg (black line). Red Dashed Curve: transmission between two parallel polarizers  $Q=1$  to  $Q=1$  with the HWP axis at 90 deg (or equivalently  $Q=-1$  to  $Q=-1$  with the HWP axis at 0). Red and Black Lower Curve: transmission with the HWP axis at 0 deg between two perpendicular polarizers. *Right:* predicted modulation efficiency (as a function of frequency), obtained as  $(T_{copol} - T_{xpol}) / (T_{copol} + T_{xpol})$ . Note that the y-axis scale ranges from 0.8 to 1.



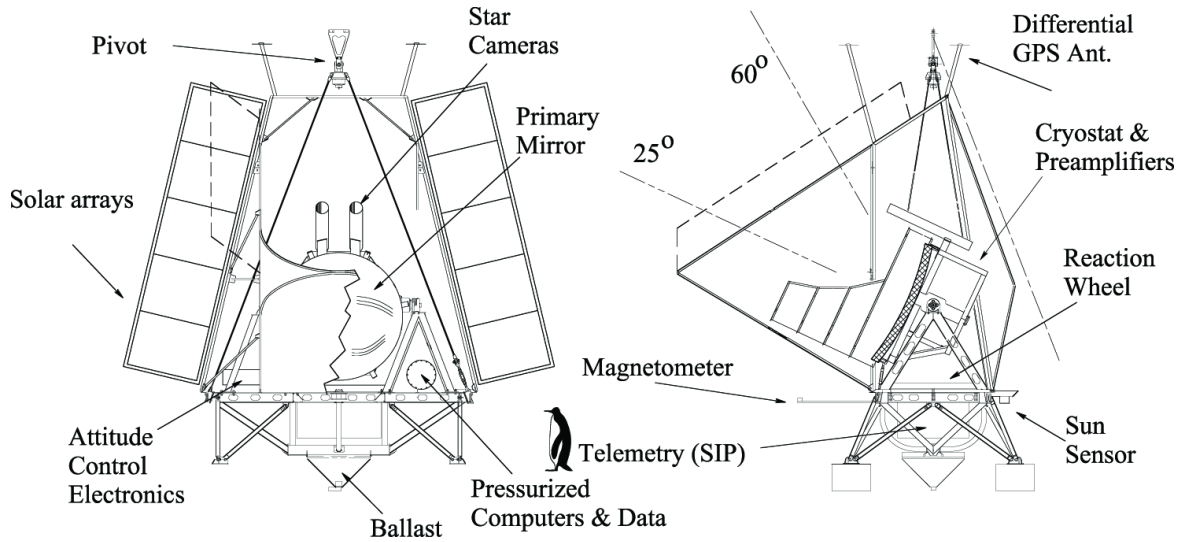


Figure 6. Front and side schematic drawings of the BLAST gondola. A 1-m tall Emperor penguin is shown for scale. The inner frame, which can be pointed in elevation, consists of the two star cameras, the telescope and its light baffle, the receiver cryostat, and associated electronics. The telescope baffles and sunshields have been updated for BLAST-Pol.

### 3.4 Cryogenics

The receiver consists of an optical cavity inside a long hold-time liquid-nitrogen and liquid-helium cryostat. Both the nitrogen and helium are maintained at slightly more than atmospheric pressure during the flight to minimize loss due to pressure drop at altitude. A  $^3\text{He}$  refrigerator maintains the detectors at 300 mK during flight. The self-contained, recycling refrigerator can maintain a base temperature of 280 mK with  $30\ \mu\text{W}$  of cooling power for 4 days. It can be recycled within 2 hr. The  $^3\text{He}$  refrigerator uses a pumped  $^4\text{He}$  pot at  $\sim 1\ \text{K}$  for cycling and to increase the hold time of the system. The pumped pot maintains 1 K with 20 mW of cooling power with outside pressure 15 Torr or less. The entire optics box containing the re-imaging optics is also cooled to 1 K.

### 3.5 Gondola

The BLAST-Pol gondola provides a pointed platform for the telescope and attaches to the balloon flight train. The gondola consists of two parts: an outer aluminum frame, which can be pointed in azimuth; and an inner aluminum frame which points in elevation. Figure 6 shows a schematic layout of the BLAST gondola with several features labelled.

The outer frame is a suspended from a  $1.1 \times 10^6\ \text{m}^3$  helium balloon, provided by NASA's Columbia Scientific Balloon Facility, through a steel cable ladder and parachute. Control systems, including flight computers and telemetry systems are mounted on the outer frame. Data are stored on solid state disks on the computers. Some portion of the data can be transmitted to a ground station by satellite links. The inner frame houses the mirrors, the receiver, the receiver read-out electronics and primary pointing sensors. These are all rigidly mounted with respect to each other on the inner frame in order to ensure that mechanical alignment is maintained throughout the flight.

To avoid large thermal changes in the optics both the inner and outer frames have attached sunshield structures. Figure 7 shows the BLAST-Pol sunshields. Shields on the outer frame are constructed from aluminized mylar and mounted on an aluminum frame, and are similar to those used in previous BLAST flights. In addition, for BLAST-Pol we have constructed new shields which are attached to a carbon fiber frame and are mounted to the inner frame. This 4-m shield will allow us to point the telescope to within  $45^\circ$  of the Sun, in order to observe targets close to the Galactic Center.

Telescope pointing is controlled by three motors. The azimuth pointing is controlled by a brushless, direct drive servo motor attached to a high moment of inertia reaction wheel, and an active pivot motor which connects

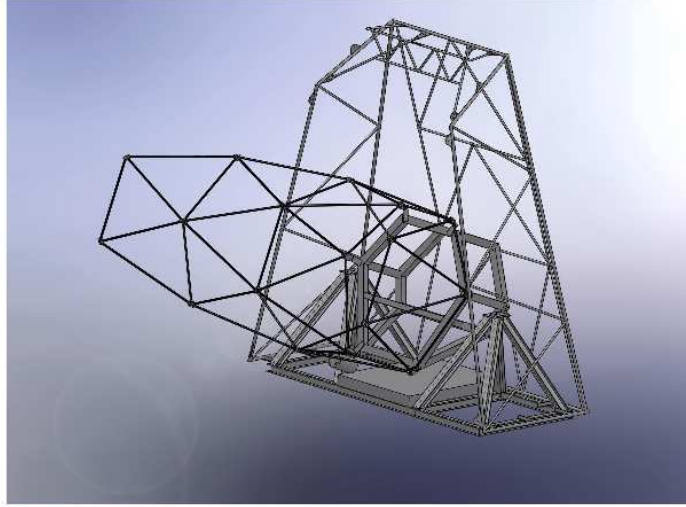


Figure 7. A drawing of the BLAST-Pol gondola showing just the inner and outer frame gondola structures, including the new inner frame sun shields which will allow the telescope to point to an azimuth distance of  $45^\circ$  from the Sun.

the cable suspended gondola to the balloon flight train. The reaction wheel consists of a 1.5-m disk made of 7.6 cm thick aluminum honeycomb, with 48 0.9 kg brass disks mounted around the perimeter. The reaction wheel is mounted at the center of mass of the telescope, directly beneath the active pivot. By spinning the reaction wheel angular momentum can be transferred to and from the gondola, allowing precise control over the azimuth velocity of the telescope with minimal latency. The active pivot motor provides additional azimuthal torque by twisting the flight train, and can also be used over long time scales to transfer angular momentum to the balloon.

The elevation of the inner frame is controlled by a servo motor mounted on one side of the inner frame at the attachment point to the outer frame. A free bearing provides the connection point between the inner and outer frames, on the other side.

In-flight pointing is measured to an accuracy of  $\sim 30''$  by a number of fine and coarse pointing sensors. These include fiber optic gyroscopes, optical star cameras, a differential GPS, an elevation encoder, inclinometers, a magnetometer and a Sun sensor. Post-flight pointing reconstruction uses only the gyroscopes and day-time star camera.<sup>50</sup> The algorithm is based on a similar multiplicative extended Kalman filter<sup>51</sup> technique used by WMAP,<sup>52</sup> which has been modified<sup>53</sup> to allow for the evaluation of the star camera and gyroscope alignment parameters. The offset between the star cameras and the submm telescope will be measured by repeated observations of pointing calibrators throughout the flight. For the BLAST06 flight it was found that the relative pointing between the star cameras and telescope varied as a function of the inner frame elevation, requiring elevation dependent corrections to pitch and yaw with scales of  $\sim 125''$  and  $\sim 20''$ , respectively. Post flight absolute pointing accuracy for BLAST06 was found to be  $< 2''$ , and random pointing errors were found to be  $< 3''$  rms.<sup>2,54</sup>

## ACKNOWLEDGMENTS

The BLAST collaboration acknowledges the support of NASA through grant numbers NAG5-12785, NAG5-13301 and NNGO-6GI11G, the Canadian Space Agency (CSA), the Science and Technology Facilities Council (STFC), Canada's Natural Sciences and Engineering Research Council (NSERC), the Canada Foundation for Innovation, the Ontario Innovation Trust, the Puerto Rico Space Grant Consortium, the Fondo Institucional para la Investigacion of the University of Puerto Rico, and the National Science Foundation Office of Polar Programs; C. B. Netterfield also acknowledges support from the Canadian Institute for Advanced Research. L. Olmi would like to acknowledge Pietro Bolli for his help with Physical Optics simulations during the testing phase of BLAST06. We would also like to thank the Columbia Scientific Balloon Facility (CSBF) staff for their

outstanding work, Dan Swetz for buliding the Fourier transform spectrometer, and Luke Bruneaux, Kyle Lepage, Danica Marsden, Vjera Miovic, and James Watt for their contribution to the project.

## REFERENCES

- [1] Griffin, M. J., Swinyard, B. M., and Vigroux, L. G., “SPIRE - Herschel’s Submillimetre Camera and Spectrometer,” in *[IR Space Telescopes and Instruments. Edited by John C. Mather . Proceedings of the SPIE]*, **4850**, 686–697 (Mar. 2003).
- [2] Pascale, E., Ade, P. A. R., Bock, J. J., Chapin, E. L., Chung, J., Devlin, M. J., Dicker, S., Griffin, M., Gundersen, J. O., Halpern, M., Hargrave, P. C., Hughes, D. H., Klein, J., MacTavish, C. J., Marsden, G., Martin, P. G., Martin, T. G., Mauskopf, P., Netterfield, C. B., Olmi, L., Patanchon, G., Rex, M., Scott, D., Semisch, C., Thomas, N., Truch, M. D. P., Tucker, C., Tucker, G. S., Viero, M. P., and Wiebe, D. V., “The Balloon-borne Large Aperture Submillimeter Telescope: BLAST,” *ApJ* **681**, 400–414 (July 2008).
- [3] Devlin, M. J., Ade, P. A. R., Aretxaga, I., Bock, J. J., Chapin, E. L., Griffin, M., Gundersen, J. O., Halpern, M., Hargrave, P. C., Hughes, D. H., Klein, J., Marsden, G., Martin, P. G., Mauskopf, P., Moncelsi, L., Netterfield, C. B., Ngo, H., Olmi, L., Pascale, E., Patanchon, G., Rex, M., Scott, D., Semisch, C., Thomas, N., Truch, M. D. P., Tucker, C., Tucker, G. S., Viero, M. P., and Wiebe, D. V., “Over half of the far-infrared background light comes from galaxies at  $z \geq 1.2$ ,” *Nature* **458**, 737–739 (Apr. 2009).
- [4] Marsden, G., Ade, P. A. R., Bock, J. J., Chapin, E. L., Devlin, M. J., Dicker, S. R., Griffin, M., Gundersen, J. O., Halpern, M., Hargrave, P. C., Hughes, D. H., Klein, J., Mauskopf, P., Magnelli, B., Moncelsi, L., Netterfield, C. B., Ngo, H., Olmi, L., Pascale, E., Patanchon, G., Rex, M., Scott, D., Semisch, C., Thomas, N., Truch, M. D. P., Tucker, C., Tucker, G. S., Viero, M. P., and Wiebe, D. V., “BLAST: Resolving the Cosmic Submillimeter Background,” *ApJ* **707**, 1729–1739 (Dec. 2009).
- [5] Pascale, E., Ade, P. A. R., Bock, J. J., Chapin, E. L., Devlin, M. J., Dye, S., Eales, S. A., Griffin, M., Gundersen, J. O., Halpern, M., Hargrave, P. C., Hughes, D. H., Klein, J., Marsden, G., Mauskopf, P., Moncelsi, L., Ngo, H., Netterfield, C. B., Olmi, L., Patanchon, G., Rex, M., Scott, D., Semisch, C., Thomas, N., Truch, M. D. P., Tucker, C., Tucker, G. S., Viero, M. P., and Wiebe, D. V., “BLAST: A Far-Infrared Measurement of the History of Star Formation,” *ApJ* **707**, 1740–1749 (Dec. 2009).
- [6] Patanchon, G., Ade, P. A. R., Bock, J. J., Chapin, E. L., Devlin, M. J., Dicker, S. R., Griffin, M., Gundersen, J. O., Halpern, M., Hargrave, P. C., Hughes, D. H., Klein, J., Marsden, G., Mauskopf, P., Moncelsi, L., Netterfield, C. B., Olmi, L., Pascale, E., Rex, M., Scott, D., Semisch, C., Thomas, N., Truch, M. D. P., Tucker, C., Tucker, G. S., Viero, M. P., and Wiebe, D. V., “Submillimeter Number Counts from Statistical Analysis of BLAST Maps,” *ApJ* **707**, 1750–1765 (Dec. 2009).
- [7] Viero, M. P., Ade, P. A. R., Bock, J. J., Chapin, E. L., Devlin, M. J., Griffin, M., Gundersen, J. O., Halpern, M., Hargrave, P. C., Hughes, D. H., Klein, J., MacTavish, C. J., Marsden, G., Martin, P. G., Mauskopf, P., Moncelsi, L., Negrello, M., Netterfield, C. B., Olmi, L., Pascale, E., Patanchon, G., Rex, M., Scott, D., Semisch, C., Thomas, N., Truch, M. D. P., Tucker, C., Tucker, G. S., and Wiebe, D. V., “BLAST: Correlations in the Cosmic Far-Infrared Background at 250, 350, and 500  $\mu\text{m}$  Reveal Clustering of Star-forming Galaxies,” *ApJ* **707**, 1766–1778 (Dec. 2009).
- [8] Wiebe, D. V., Ade, P. A. R., Bock, J. J., Chapin, E. L., Devlin, M. J., Dicker, S., Griffin, M., Gundersen, J. O., Halpern, M., Hargrave, P. C., Hughes, D. H., Klein, J., Marsden, G., Martin, P. G., Mauskopf, P., Netterfield, C. B., Olmi, L., Pascale, E., Patanchon, G., Rex, M., Scott, D., Semisch, C., Thomas, N., Truch, M. D. P., Tucker, C., Tucker, G. S., and Viero, M. P., “BLAST Observations of Resolved Galaxies: Temperature Profiles and the Effect of Active Galactic Nuclei on FIR to Submillimeter Emission,” *ApJ* **707**, 1809–1823 (Dec. 2009).
- [9] Netterfield, C. B., Ade, P. A. R., Bock, J. J., Chapin, E. L., Devlin, M. J., Griffin, M., Gundersen, J. O., Halpern, M., Hargrave, P. C., Hughes, D. H., Klein, J., Marsden, G., Martin, P. G., Mauskopf, P., Olmi, L., Pascale, E., Patanchon, G., Rex, M., Roy, A., Scott, D., Semisch, C., Thomas, N., Truch, M. D. P., Tucker, C., Tucker, G. S., Viero, M. P., and Wiebe, D. V., “BLAST: The Mass Function, Lifetimes, and Properties of Intermediate Mass Cores from a 50 deg<sup>2</sup> Submillimeter Galactic Survey in Vela (ell  $\sim 265^\circ$ ),” *ApJ* **707**, 1824–1835 (Dec. 2009).
- [10] McKee, C. F. and Ostriker, E. C., “Theory of Star Formation,” *ARA&A* **45**, 565–687 (Sept. 2007).

- [11] Crutcher, R. M., Nutter, D. J., Ward-Thompson, D., and Kirk, J. M., “SCUBA Polarization Measurements of the Magnetic Field Strengths in the L183, L1544, and L43 Prestellar Cores,” *ApJ* **600**, 279–285 (Jan. 2004).
- [12] Whittet, D. C. B., Hough, J. H., Lazarian, A., and Hoang, T., “The Efficiency of Grain Alignment in Dense Interstellar Clouds: a Reassessment of Constraints from Near-Infrared Polarization,” *ApJ* **674**, 304–315 (Feb. 2008).
- [13] Hildebrand, R. H., Davidson, J. A., Dotson, J. L., Dowell, C. D., Novak, G., and Vaillancourt, J. E., “A Primer on Far-Infrared Polarimetry,” *PASP* **112**, 1215–1235 (Sept. 2000).
- [14] Ward-Thompson, D., Kirk, J. M., Crutcher, R. M., Greaves, J. S., Holland, W. S., and André, P., “First Observations of the Magnetic Field Geometry in Prestellar Cores,” *ApJ* **537**, L135–L138 (July 2000).
- [15] Lamarre, J. M., Puget, J. L., Bouchet, F., Ade, P. A. R., Benoit, A., Bernard, J. P., Bock, J., de Bernardis, P., Charra, J., Couchot, F., Delabrouille, J., Efstathiou, G., Giard, M., Guyot, G., Lange, A., Maffei, B., Murphy, A., Pajot, F., Piat, M., Ristorcelli, I., Santos, D., Sudiwala, R., Sygnet, J. F., Torre, J. P., Yurchenko, V., and Yvon, D., “The Planck High Frequency Instrument, a third generation CMB experiment, and a full sky submillimeter survey,” *New Astronomy Review* **47**, 1017–1024 (Dec. 2003).
- [16] Li, H., Griffin, G. S., Krejny, M., Novak, G., Loewenstein, R. F., Newcomb, M. G., Calisse, P. G., and Chuss, D. T., “Results of SPARO 2003: Mapping Magnetic Fields in Giant Molecular Clouds,” *ApJ* **648**, 340–354 (Sept. 2006).
- [17] Novak, G., Dotson, J. L., and Li, H., “Dispersion of Observed Position Angles of Submillimeter Polarization in Molecular Clouds,” *ApJ* **695**, 1362–1369 (Apr. 2009).
- [18] Ostriker, E. C., Stone, J. M., and Gammie, C. F., “Density, Velocity, and Magnetic Field Structure in Turbulent Molecular Cloud Models,” *ApJ* **546**, 980–1005 (Jan. 2001).
- [19] Jones, C. E. and Basu, S., “The Intrinsic Shapes of Molecular Cloud Fragments over a Range of Length Scales,” *ApJ* **569**, 280–287 (Apr. 2002).
- [20] Mouschovias, T. C. and Ciolek, G. E., “Magnetic Fields and Star Formation: A Theory Reaching Adulthood,” in [*NATO ASIC Proc. 540: The Origin of Stars and Planetary Systems*], Lada, C. J. and Kylafis, N. D., eds., 305–+ (1999).
- [21] Allen, A., Li, Z.-Y., and Shu, F. H., “Collapse of Magnetized Singular Isothermal Toroids. II. Rotation and Magnetic Braking,” *ApJ* **599**, 363–379 (Dec. 2003).
- [22] Tassis, K., Dowell, C. D., Hildebrand, R. H., Kirby, L., and Vaillancourt, J. E., “Statistical Assessment of Shapes and Magnetic Field Orientations in Molecular Clouds through Polarization Observations,” *MNRAS* **399**, 1681–1693 (Nov. 2009).
- [23] Heyer, M., Gong, H., Ostriker, E., and Brunt, C., “Magnetically Aligned Velocity Anisotropy in the Taurus Molecular Cloud,” *ApJ* **680**, 420–427 (June 2008).
- [24] Goldsmith, P. F., Heyer, M., Narayanan, G., Snell, R., Li, D., and Brunt, C., “Large-Scale Structure of the Molecular Gas in Taurus Revealed by High Linear Dynamic Range Spectral Line Mapping,” *ApJ* **680**, 428–445 (June 2008).
- [25] Goodman, A. A., Bastien, P., Menard, F., and Myers, P. C., “Optical polarization maps of star-forming regions in Perseus, Taurus, and Ophiuchus,” *ApJ* **359**, 363–377 (Aug. 1990).
- [26] Cho, J. and Lazarian, A., “Grain Alignment by Radiation in Dark Clouds and Cores,” *ApJ* **631**, 361–370 (Sept. 2005).
- [27] Alves, F. O., Franco, G. A. P., and Girart, J. M., “Optical polarimetry toward the Pipe nebula: revealing the importance of the magnetic field,” *A&A* **486**, L13–L16 (Aug. 2008).
- [28] Chandrasekhar, S. and Fermi, E., “Magnetic Fields in Spiral Arm,” *ApJ* **118**, 113 (July 1953).
- [29] Zweibel, E. G., “Magnetic field-line tangling and polarization measurements in clumpy molecular gas,” *ApJ* **362**, 545–550 (Oct. 1990).
- [30] Pelkonen, V.-M., Juvela, M., and Padoan, P., “Simulations of polarized dust emission,” *A&A* **461**, 551–564 (Jan. 2007).
- [31] Falceta-Gonçalves, D., Lazarian, A., and Kowal, G., “Studies of Regular and Random Magnetic Fields in the ISM: Statistics of Polarization Vectors and the Chandrasekhar-Fermi Technique,” *ApJ* **679**, 537–551 (May 2008).

- [32] Bethell, T. J., Chepurnov, A., Lazarian, A., and Kim, J., “Polarization of Dust Emission in Clumpy Molecular Clouds and Cores,” *ApJ* **663**, 1055–1068 (July 2007).
- [33] Vaillancourt, J. E., Dowell, C. D., Hildebrand, R. H., Kirby, L., Krejny, M. M., Li, H.-b., Novak, G., Houde, M., Shinnaga, H., and Attard, M., “New Results on the Submillimeter Polarization Spectrum of the Orion Molecular Cloud,” *ApJ* **679**, L25–L28 (May 2008).
- [34] Hu, W. and White, M., “A CMB polarization primer,” *New Astronomy* **2**, 323–344 (Oct. 1997).
- [35] Kamionkowski, M., Kosowsky, A., and Stebbins, A., “Statistics of cosmic microwave background polarization,” *Phys. Rev. D* **55**, 7368–7388 (Jun 1997).
- [36] Zaldarriaga, M. and Seljak, U. c. v., “All-sky analysis of polarization in the microwave background,” *Phys. Rev. D* **55**, 1830–1840 (Feb 1997).
- [37] Page, L., Hinshaw, G., Komatsu, E., Nolte, M. R., Spergel, D. N., Bennett, C. L., Barnes, C., Bean, R., Doré, O., Dunkley, J., Halpern, M., Hill, R. S., Jarosik, N., Kogut, A., Limon, M., Meyer, S. S., Odegard, N., Peiris, H. V., Tucker, G. S., Verde, L., Weiland, J. L., Wollack, E., and Wright, E. L., “Three-Year Wilkinson Microwave Anisotropy Probe (WMAP) Observations: Polarization Analysis,” *ApJS* **170**, 335–376 (June 2007).
- [38] Benoît, A., Ade, P., Amblard, A., Ansari, R., Aubourg, É., Bargout, S., Bartlett, J. G., Bernard, J.-P., Bhatia, R. S., Blanchard, A., Bock, J. J., Boscaleri, A., Bouchet, F. R., Bourrachot, A., Camus, P., Couchot, F., de Bernardis, P., Delabrouille, J., Désert, F.-X., Doré, O., Douspis, M., Dumoulin, L., Dupac, X., Filliatre, P., Fosalba, P., Ganga, K., Gannaway, F., Gautier, B., Giard, M., Giraud-Héraud, Y., Gispert, R., Guglielmi, L., Hamilton, J.-C., Hanany, S., Henrot-Versillé, S., Kaplan, J., Lagache, G., Lamarre, J.-M., Lange, A. E., Macías-Pérez, J. F., Madet, K., Maffei, B., Magneville, C., Marrone, D. P., Masi, S., Mayet, F., Murphy, A., Naraghi, F., Nati, F., Patanchon, G., Perrin, G., Piat, M., Ponthieu, N., Prunet, S., Puget, J.-L., Renault, C., Rosset, C., Santos, D., Starobinsky, A., Strukov, I., Sudiwala, R. V., Teyssier, R., Tristram, M., Tucker, C., Vanel, J.-C., Vibert, D., Wakui, E., and Yvon, D., “First detection of polarization of the submillimetre diffuse galactic dust emission by Archeops,” *A&A* **424**, 571–582 (Sept. 2004).
- [39] Finkbeiner, D. P., Davis, M., and Schlegel, D. J., “Extrapolation of Galactic Dust Emission at 100 Microns to Cosmic Microwave Background Radiation Frequencies Using FIRAS,” *ApJ* **524**, 867–886 (Oct. 1999).
- [40] Ade, P. A. R., Pisano, G., Tucker, C., and Weaver, S., “A review of metal mesh filters,” in [*Society of Photo-Optical Instrumentation Engineers (SPIE) Conference Series*], *Society of Photo-Optical Instrumentation Engineers (SPIE) Conference Series* **6275** (July 2006).
- [41] Olmi, L., “Optical designs for submillimeter-wave spherical-primary (sub)orbital telescopes and novel optimization techniques,” in [*Highly Innovative Space Telescope Concepts Edited by Howard A. MacEwen. Proceedings of the SPIE*], **4849**, 245–256 (Dec. 2002).
- [42] Glenn, J., Bock, J. J., Chattopadhyay, G., Edgington, S. F., Lange, A. E., Zmuidzinas, J., Mauskopf, P. D., Rownd, B., Yuen, L., and Ade, P. A., “Bolocam: a millimeter-wave bolometric camera,” in [*Proc. SPIE, Advanced Technology MMW, Radio, and Terahertz Telescopes, Thomas G. Phillips; Ed.*], **3357**, 326–334 (July 1998).
- [43] Rownd, B., Bock, J. J., Chattopadhyay, G., Glenn, J., and Griffin, M. J., “Design and performance of feedhorn-coupled bolometer arrays for SPIRE,” in [*Millimeter and Submillimeter Detectors for Astronomy. Edited by Phillips, Thomas G.; Zmuidzinas, Jonas. Proceedings of the SPIE*], **4855**, 510–519 (Feb. 2003).
- [44] Hanany, S., Hubmayr, J., Johnson, B. R., Matsumura, T., Oxley, P., and Thibodeau, M., “Millimeter-wave achromatic half-wave plate,” *Appl. Opt.* **44**, 4666–4670 (Aug. 2005).
- [45] Savini, G., Pisano, G., and Ade, P. A. R., “Achromatic half-wave plate for submillimeter instruments in cosmic microwave background astronomy: modeling and simulation,” *Appl. Opt.* **45**, 8907–8915 (Dec. 2006).
- [46] Pisano, G., Savini, G., Ade, P. A. R., Haynes, V., and Gear, W. K., “Achromatic half-wave plate for submillimeter instruments in cosmic microwave background astronomy: experimental characterization,” *Appl. Opt.* **45**, 6982–6989 (Sept. 2006).
- [47] Johnson, B. R., Collins, J., Abroe, M. E., Ade, P. A. R., Bock, J., Borrill, J., Boscaleri, A., de Bernardis, P., Hanany, S., Jaffe, A. H., Jones, T., Lee, A. T., Levinson, L., Matsumura, T., Rabi, B., Renbarger, T., Richards, P. L., Smoot, G. F., Stompor, R., Tran, H. T., Winant, C. D., Wu, J. H. P., and Zuntz, J., “MAXIPOL: Cosmic Microwave Background Polarimetry Using a Rotating Half-Wave Plate,” *ApJ* **665**, 42–54 (Aug. 2007).

- [48] Zhang, J., Ade, P. A. R., Mauskopf, P., Moncelsi, L., Savini, G., and Whitehouse, N., “New artificial dielectric metamaterial and its application as a terahertz antireflection coating,” *Appl. Opt.* **48**, 6635–+ (Dec. 2009).
- [49] Renbarger, T., Chuss, D. T., Dotson, J. L., Griffin, G. S., Hanna, J. L., Loewenstein, R. F., Malhotra, P. S., Marshall, J. L., Novak, G., and Pernic, R. J., “Early Results from SPARO: Instrument Characterization and Polarimetry of NGC 6334,” *PASP* **116**, 415–424 (May 2004).
- [50] Rex, M., Chapin, E., Devlin, M. J., Gundersen, J., Klein, J., Pascale, E., and Wiebe, D., “BLAST autonomous daytime star cameras,” in [*Ground-based and Airborne Instrumentation for Astronomy. Edited by McLean, Ian S.; Iye, Masanori. Proceedings of the SPIE, Volume 6269, pp. 62693H (2006).*], *Presented at the Society of Photo-Optical Instrumentation Engineers (SPIE) Conference* **6269** (July 2006).
- [51] Markley, F. L., “Attitude Error Representations for Kalman Filtering,” *Journal of Guidance, Control, and Dynamics* **26**, 311–317 (2003).
- [52] Harman, R. R., “Wilkinson Microwave Anisotropy Probe (WMAP) Attitude Estimation Filter Comparison,” tech. rep., Flight Mechanics Symposium; Greenbelt, MD (2005).
- [53] Pittelkau, M. E., “Kalman Filtering for Spacecraft System Alignment Calibration,” *Journal of Guidance, Control, and Dynamics* **24**, 1187–1195 (2001).
- [54] Marsden, G., Ade, P. A. R., Benton, S., Bock, J. J., Chapin, E. L., Chung, J., Devlin, M. J., Dicker, S., Fissel, L., Griffin, M., Gundersen, J. O., Halpern, M., Hargrave, P. C., Hughes, D. H., Klein, J., Korotkov, A., MacTavish, C. J., Martin, P. G., Martin, T. G., Matthews, T. G., Mauskopf, P., Moncelsi, L., Netterfield, C. B., Novak, G., Pascale, E., Olmi, L., Patanchon, G., Rex, M., Savini, G., Scott, D., Semisch, C., Thomas, N., Truch, M. D. P., Tucker, C., Tucker, G. S., Viero, M. P., Ward-Thompson, D., and Wiebe, D. V., “The Balloon-borne Large-Aperture Submillimeter Telescope for polarization: BLAST-pol,” in [*Society of Photo-Optical Instrumentation Engineers (SPIE) Conference Series*], *Society of Photo-Optical Instrumentation Engineers (SPIE) Conference Series* **7020** (Aug. 2008).